EuroIntervention 2015;10:1169-1177 published online ahead of print May 2014

Absorb everolimus-eluting bioresorbable scaffolds in coronary bifurcations: a bench study of deployment, side branch dilatation and post-dilatation strategies

John A. Ormiston[1,2,3]*, MBChB; Bruce Webber[1], MHSc; Ben Ubod[1], BSN; Mark W.I. Webster[1,2,3], MBChB; Jonathon White[2], MBChB

1. Mercy Angiography, Auckland, New Zealand; 2. Auckland City Hospital, Auckland, New Zealand; 3. University of Auckland School of Medicine, Auckland, New Zealand

KEYWORDS

- bifurcations
- bioresorbable scaffold
- coronary artery disease
- coronary intervention
- stenting

Abstract

Aims: To provide bench insights which may predict safety and efficacy of side branch dilatation (SB) and kissing balloon post-dilatation (KBPD) in Absorb everolimus-eluting bioresorbable scaffolds deployed in bifurcations.

Methods and results: Stages of deployment and post-dilatation of scaffolds (3.0 and 3.5 mm diameter) in bifurcation phantoms were imaged by fluoroscopy, light microscopy and micro-computed tomography. Dilatation through the scaffold side displaced struts from the side branch (SB) lumen, but caused main branch (MB) malapposition opposite the SB, MB scaffold narrowing beyond the SB, and protrusion of struts into the SB. Scaffold distortion was corrected by MB post-dilatation or by mini-kissing balloon post-dilatation (mini-KBPD). When 3.0 mm diameter balloons were used for SB dilatation or mini-KBPD in 3.0 mm Absorbs, strut fracture did not occur at or below inflation pressures of 10 and 5 atm, respectively. Above these thresholds, the likelihood of strut fracture increased with increasing pressure. Fractures were usually single without malapposition, but mini-KBPD or post-dilatation with high inflation pressures sometimes caused multiple strut fractures and lumen compromise.

Conclusions: SB dilatation of an Absorb caused MB distortion which was corrected by MB post-dilation or low-pressure mini-KBPD without scaffold damage below pressure thresholds. These benchtop insights may help guide the clinical deployment of Absorb scaffolds in bifurcations and might enhance clinical outcomes but need clinical confirmation.

**Corresponding author: Mercy Angiography, Mercy Hospital, 98 Mountain Road, Epsom, PO Box 9911, Newmarket 1023, New Zealand. E-mail: johno@mercyangiography.co.nz*

SUBMITTED ON 09/03/2014 - REVISION RECEIVED ON 18/04/2014 - ACCEPTED ON 23/04/2014

DOI: 10.4244/EIJY14M05_08

Introduction

The Absorb bioresorbable everolimus-eluting scaffold (Abbott Vascular, Santa Clara, CA, USA) has been clinically evaluated in relatively simple lesions[1,2]. There are limited data concerning its use in coronary bifurcations, with recent reports showing that SB dilatation of an Absorb causes distortion similar to that seen in metallic stents[3-7]. While main branch (MB) post-dilatation and KBPD can correct metallic stent distortion[7,8], the efficacy and safety of post-dilatation strategies for Absorb distortion are uncertain. Because oversized balloon post-dilatation in a patient with a non-bifurcation lesion ruptured multiple Absorb struts[9], there are concerns that the simultaneous inflation of two balloons during KBPD may cause significant scaffold damage.

This bench study assessed SB dilatation between struts in Absorb scaffolds with different balloon sizes, different inflation pressures and different SB angles, and evaluated strategies both qualitatively and quantitatively that might be used to correct scaffold distortion. We aimed to provide recommendations for safe scaffold post-dilatation, including safe KBPD.

Methods

SCAFFOLD DESIGN

The Absorb scaffold **(Figure 1)** has in-phase sinusoidal hoops with three straight longitudinal connectors linking adjacent peaks and valleys. Manufacturer-supplied measurements for a 3.0 mm scaffold indicate a thickness (radial direction) for all hoops and connectors of 157 microns. The connector diameter in the circumferential direction (140 microns) is less than the hoop diameter (191 microns). These measurements include the resorbable coating which contains and controls the release of the antiproliferative drug, everolimus (Novartis, Basel, Switzerland). Another manufacturer-supplied measurement which influences SB post-dilatation and the potential for strut fracture is the perimeter of a cell (**Figure 1**, broken red line), which is less for the 2.5/3.0 mm (9.4 mm) scaffolds than the 3.5 mm scaffold (11.4 mm). The calculated potential circular diameter of a cell is 3.0 mm for the 2.5/3.0 mm scaffold and 3.6 mm for the 3.5 mm scaffold.

Because of the risk of strut fracture, the instructions for use of Absorb scaffolds limit post-dilation to 0.5 mm greater than each scaffold's nominal diameter and mandate slow inflation.

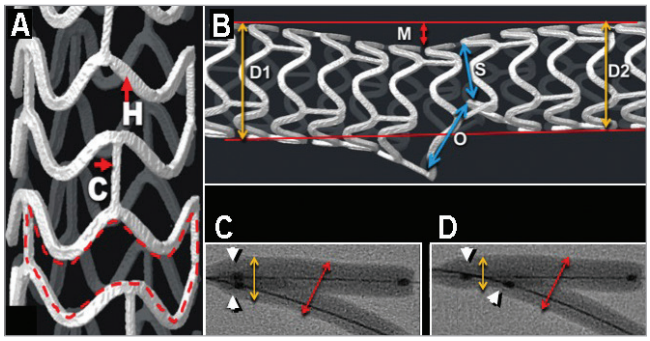

Figure 1. *Absorb scaffold design, distortion with side branch dilatation and balloon diameters with kissing balloon post-dilatation. A) A micro-CT image of the Absorb scaffold. In-phase sinusoidal hoops (H) are linked by three straight connectors (C) which join the peaks and valleys of the hoops. The broken red line delineates a scaffold cell. B) A micro-CT of a 3.5 mm Absorb scaffold after SB dilatation with a 3.0 mm balloon showing distortion and the principles of distortion measurement. M: main branch malapposition; O: side branch ostium; S: scaffold narrowing; D1: proximal reference diameter; D2: distal reference diameter. C) & D) Radiographic images of KBPD (C) and mini-KBPD (D). The white arrowheads indicate the proximal balloon markers which overlap for conventional KBPD and are offset for mini-KBPD. The red double arrows show the site of maximum balloon diameter measurement and the yellow double arrows show the proximal diameter.*

TEST APPARATUS AND TEST METHOD

To examine different bifurcation strategies, 3.0 and 3.5 mm Absorb scaffolds were deployed in the MB of silicone phantoms with "B" angles[10] between the MB and SB of 30°, 60°, or 90°. The MB phantom diameter was 3.5 mm tapering to 3.0 mm distal to the SB origin, and the SB diameter was 3.0 mm. All deployments were carried out in an aqueous bath at 37°C. All balloon dilatations were with non-compliant (NC) balloons. The different deployment and post-dilatation sequences tested were observed and recorded fluoroscopically and recorded by photography using an EOSO-1 D Canon digital camera (Canon, Inc., Tokyo, Japan) with a Leica Z6 APO microscopic lens (Leica Microsystems, Wetzlar, Germany). Measurements were made from photographs using Image-Pro Plus software version 7.0.0.591 (Media Cybernetics, Inc., Rockville, MD, USA). Calibration was with a graticule of known dimensions photographed in the plane of the stent. In addition, scaffolds were imaged using micro-computed tomography (micro-CT) (SkyScan 1172; SkyScan/Bruker-microCT, Kontich, Belgium). All experiments were conducted in phantoms except for some where, in order to illustrate fractures, no phantom was used to facilitate quality light photography.

SINGLE SCAFFOLD DEPLOYMENT AND GENERAL POST-DILATATION STRATEGY

The scaffold deployment strategy **(Figure 2)** was a modification of the European Bifurcation Club (EBC) recommendations for single metallic stent deployment with SB dilatation and KBPD[11]. After wiring both branches and in contrast to the EBC recommendations, we sized the scaffold to the proximal MB because we wanted to post-dilatate the proximal scaffold without oversizing and risking strut fracture **(Figure 2)**. Our scaffold deployment pressure was low (5-10 atm) to avoid oversizing the distal scaffold. Following this, we carried out proximal optimisation (POT) up to the carina with a balloon sized to the proximal vessel inflated to a pressure of 15 atm. We then advanced a wire through the side of the MB scaffold to the SB. To achieve optimal scaffolding of the SB ostium[12], we aimed to cross near the carina, although we could not check this easily. Inflation of a balloon was carried out through the side of the MB scaffold into the SB at different pressures, as described in the different experiments

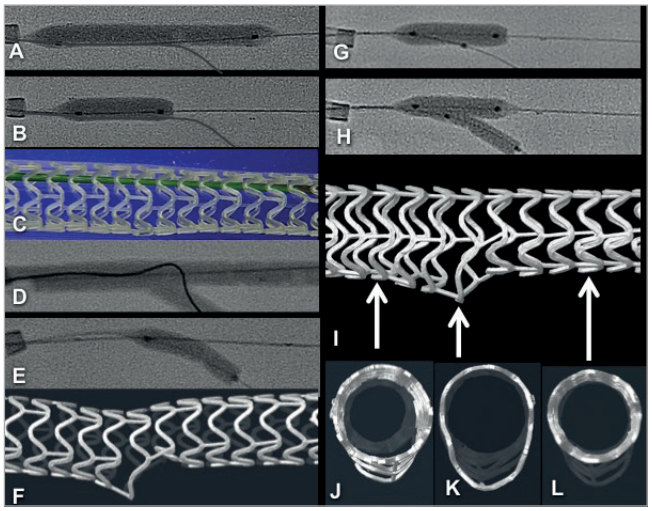

Figure 2. *General strategy for deploying a single scaffold with SB dilatation, MB post-dilatation then mini-KBPD as might be used in a provisional SB strategy. Radiographic image (A) shows deployment of a 3.5×28 mm Absorb scaffold at 5 atm in a silicone phantom where the proximal vessel is 3.5 mm, the distal MB is 3.0 mm and the SB is 3.0 mm in diameter. Wires (0.014 inch) have been placed in both branches. B) Proximal optimisation (POT) with inflation of a 3.5 mm balloon up to the carina at 15 atm. C) Photograph of a scaffold after POT. D) A wire passing from the MB to the SB through a cell close to the carina in order that ostial scaffolding is optimised after subsequent dilatations. E) A 3 mm balloon through the side of the MB scaffold inflated to 16 atmospheres, and (F) a micro-CT image after SB dilatation. G) The MB is post-dilated with a 3.5 mm non-compliant balloon to 16 atm. H) Mini-KBPD with a 3.5 mm and a 3.0 mm balloon with small overlap inflated slowly to 5 atm. The red arrow indicates a constriction on the balloon caused by a hoop that is not fractured. I) Distortion has been corrected with maintenance of SB ostial size. J) The scaffold cross-section proximally is round (due to POT), is appropriately oval at the SB origin (K) and round distally (L).*

below. This caused distortion of the MB scaffold with malapposition of the scaffold opposite the SB ostium and MB scaffold narrowing just distal to the SB ostium **(Figure 2)**. MB post-dilatation across the SB ostium with a balloon sized to the MB at 12-16 atm pressure was then performed. The scaffold was imaged to determine whether this strategy corrected scaffold distortion. Next, KBPD with minimal overlap of balloons (mini-KBPD) was carried out slowly at low pressure (5 atm) to correct distortion **(Figure 2)**. For mini-KBPD, the aim was to place the proximal marker of the side branch balloon in the main branch immediately proximal to the side branch ostium. The sites of measurements are shown in **Figure 1**.

SCAFFOLD DAMAGE WITH SB DILATATION USING BALLOONS INFLATED TO 14 ATM

To test whether SB dilatation damaged scaffolds, we deployed 3.0 and 3.5 mm Absorbs in bifurcation phantoms with the three SB angles and carried out 145 SB dilatations with 2.0, 2.5 and 3.0 mm balloons at 14 atm. The scaffolds were inspected and photographed after SB dilatation.

SCAFFOLD INTEGRITY WITH MB POST-DILATATION AFTER SB DILATATION

To test for integrity, scaffolds were inspected after MB post-dilatation which followed the SB dilatations above. We post-dilated MBs (n=80 post-dilatations) to 14 atm using 3.0 mm NC balloons for 3.0 mm scaffolds and 3.5 mm NC balloons for 3.5 mm scaffolds.

ASSESSMENT OF THE RELATIONSHIP BETWEEN SB BALLOON PRESSURE AND STRUT FRACTURE

Scaffolds 3.0 mm in diameter were deployed in the MB of a phantom with a 30° SB angle. SB dilatation was carried out with a 3.0 mm NC balloon inflated slowly up to more than 20 atm with periodic inspection for strut fracture.

ASSESSMENT OF THE RELATIONSHIP BETWEEN KBPD PRESSURE AND STRUT FRACTURE

Scaffolds 3.0 mm in diameter were deployed in the MB of a phantom with a 30° SB angle. Two 3.0 mm NC balloons were inflated slowly simultaneously up to 16 atm in scaffolds with periodic inspection for strut fracture.

SCAFFOLD DISTORTION AND STRUT FRACTURE AFTER SB DILATATION, AND AFTER DISTORTION CORRECTION STRATEGIES

Distortion was compared in 3.0 mm scaffolds deployed in phantoms with 30°, 60° and 90° SB angles using 2.0 mm, 2.5 mm and 3.0 mm SB balloons inflated to 14 atm. The MB was then post-dilated with a 3.5 mm balloon at 14 atm (POT) followed by mini-KBPD at 5 atm with the 3.5 mm balloon and a 2.0 mm, 2.5 mm, or 3.0 mm balloon. Three scaffolds were used for each series, so 27 scaffolds were used for the 27 sequences. Scaffolds were inspected and measurements (**Figure 1**, upper panel) were made after SB dilatation, MB post-dilatation and mini-KBPD. The percentage scaffold narrowing was calculated as (mean reference diameter- MB stenosis diameter) ÷ mean reference diameter ×100.

COMPARISON OF BALLOON DIAMETERS WITH KBPD AND MINI-KBPD STRATEGIES

To compare the balloon diameters with KBPD and mini-KBPD, 3.0 mm NC balloons were expanded in a silicone phantom with a 30° SB angle without scaffolds **(Figure 1)**. The maximum diameter was measured at the level of the carina and approximately perpendicular to a line bisecting the carina.

STATISTICS

The data are presented as mean ± SD. The differences in percentage scaffold stenosis (after side branch dilatation, main branch post-dilatation and mini-KBPD) between scaffolds were compared with either the Kruskal-Wallis test or Mann-Whitney U

test, depending upon the differences between scaffolds in main branch malapposition and side branch ostial diameter. Balloon diameters with KPBD and mini-KBPD were compared using the Mann-Whitney U test. Statistical analyses were performed using SAS statistical software version 9.3 (SAS Institute, Cary, NC, USA). The two-sample Z-test was used to compare the proportion of strut fractures after SB dilatation with a 2.5 or a 3.0 mm balloon. The same test was also used to compare the proportion of hoop fractures to the proportion of connector fractures. All results were from two-sided tests and a p-value of <0.05 was considered significant.

Results

SCAFFOLD DAMAGE WITH SB DILATATION USING BALLOONS INFLATED TO 14 ATM

SB dilatation in 3.0 and 3.5 mm scaffolds **(Table 1)** with 2.5 and 3.0 mm diameter NC balloons at a mean pressure of 14 atm caused strut fracture in 20 of 145 dilatations (14%). The 2.0 mm balloon did not cause fracture. There was a trend for the 3.0 mm balloon to cause more strut fracture (19%) than a 2.5 mm balloon (13%, p=0.37). The incidence of hoop fractures (8%) was similar to the incidence of connector fractures (6%, p=0.64). These fractures were single and not associated with malapposition.

RELATIONSHIP BETWEEN BALLOON PRESSURE AND SCAFFOLD STRUT FRACTURE

With SB dilatation of a 3.0 mm Absorb with a 3.0 mm NC balloon (n=24) in a phantom with a 30° SB angle, at 10 atm or less there were no strut fractures. However, at higher pressures fractures did occur **(Figure 3A)**.

RELATIONSHIP BETWEEN MINI-KBPD PRESSURE AND STRUT FRACTURE

With mini-KBPD using two 3.0 mm NC balloons in a 3.0 mm scaffold there were no strut fractures when the inflation pressure was 5 atm or less (n=32) **(Figure 3B)**. However, at higher pressures fractures occurred. At low pressure (5 atm) the scaffold constrained balloon expansion **(Figure 4)**. At higher pressure (15 atm) there was no longer balloon "waisting", as the scaffold no longer constrained balloon expansion because some scaffold struts had fractured **(Figure 4)**. In contrast to SB dilatation **(Table 1)**, all fractures caused by mini-KBPD were in hoops.

SCAFFOLD INTEGRITY FOLLOWING MB POST-DILATATION AFTER SB DILATATION

There were no strut fractures with MB post-dilatation after SB dilatation (n=80) using 3.0 mm NC balloons for 3.0 mm scaffolds and 3.5 mm NC balloons for 3.5 mm scaffolds inflated to an average of 14 atm.

SCAFFOLD INTEGRITY AND PROXIMAL OPTIMISATION TREATMENT

POT with a 3.5 mm NC balloon inflated slowly in a 3.0 mm scaffold to 14 atm (diameter from the compliance chart is 3.54 mm) did not cause strut fracture (n=27).

SCAFFOLD DISTORTION AFTER SB DILATATION, AFTER MB POST-DILATATION AND THEN AFTER MINI-KBPD

SB dilatation in a 3.0 mm diameter Absorb caused distortion with narrowing of the scaffold immediately distal to the SB, MB malapposition, some clearance of struts from the SB ostium and protrusion of struts into the SB ostium **(Figure 1)**.

Table1. Balloon diameters and strut fracture with SB dilatation at a mean of 14 atmospheres in 3.0 and 3.5 mm Absorb scaffolds with 2.0, 2.5 and 3.0 mm NC balloons.

Balloon diameter	Side dilatations (N)	Strut fracture (N)	Dilatations causing fracture (%)	Connector fracture (N)	Hoop fracture (N)
3.0 mm Absorb scaffold					
2.0 mm	18	0	0%	0	0
2.5 mm	30	4	13%	3	1
3.0 mm	64	14	22%	6	8
Total for 3.0 mm scaffolds	112	18	16%	9	9
3.5 mm Absorb scaffold					
2.0 mm	8	0	0%	0%	0
2.5 mm	10	1	10%	1	0
3.0 mm	15	1	7%	1	0
Total for 3.5 mm scaffolds	33	2	6%	2	0
3.0 and 3.5 mm scaffolds					
2.0 mm	26	0	0%	0	0
2.5 mm	40	5	13%	4	1
3.0 mm	79	15	19%	7	8
Total for both 3.0 and 3.5 mm scaffolds	145	20	14%	11 (8%)	9 (6%)

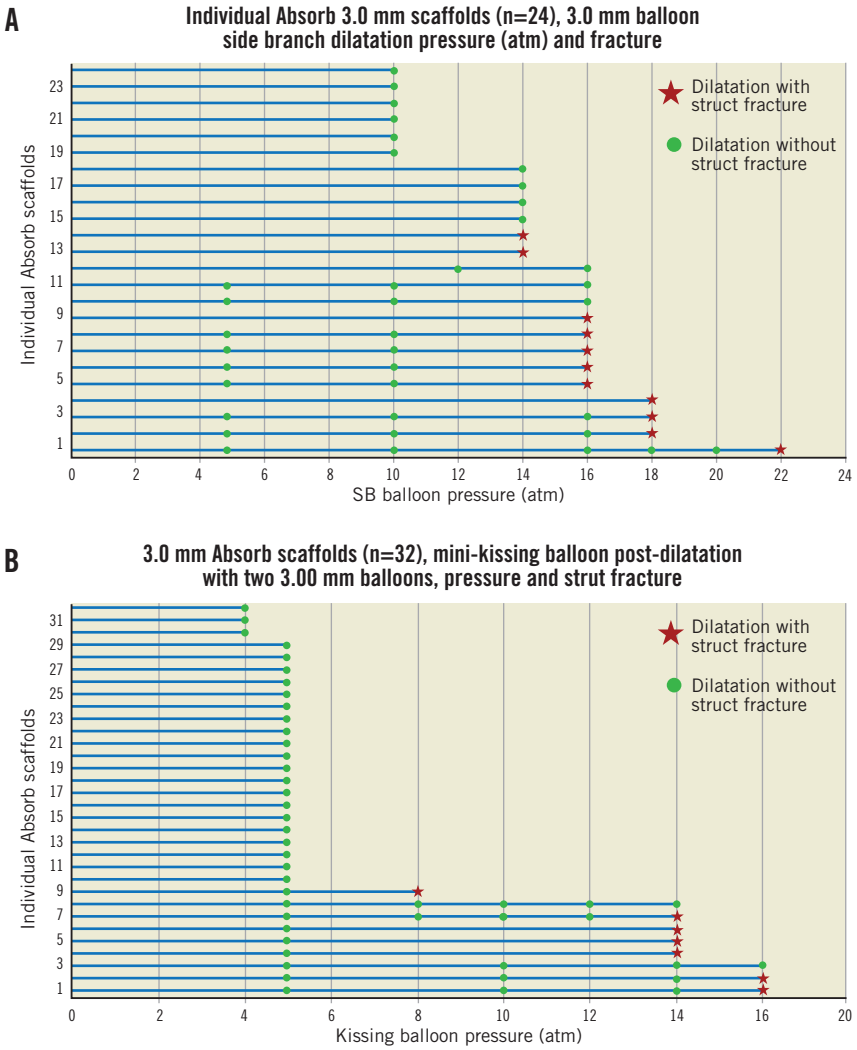

Figure 3. *Absorb scaffolds and strut fracture with side branch dilatation and mini-kissing balloon post-dilatation. Panel A summarises fractures occurring in 3.0 mm Absorb scaffolds (n=24) after side branch dilatation at different pressures with a 3.0 mm balloon. Green dots indicate the pressure at which testing and inspection were done without fracture and the red stars indicate dilatation pressure and fracture. There were no fractures at 10 atm pressure or less. Panel B is a similar representation but with mini-kissing balloon post-dilatation (two 3.0 mm balloons) in 3.0 mm Absorb scaffolds (n=32). There were no fractures at 5 atm pressure or less.*

The severity of the scaffold narrowing immediately distal to the SB **(Figure 5)** increased with increasing SB balloon diameter (Kruskal-Wallis, p=0.015). MB post-dilatation improved this scaffold narrowing, except in phantoms with a 90° SB angle where the response was variable **(Figure 5)**. Mini-KBPD appeared to improve the MB narrowing further, although the difference was not significant.

The MB scaffold malapposition **(Figure 5)** occurred with all SB balloon diameters and SB angles. There was a trend to greatest malapposition with a 3.0 mm balloon in 30° angled SB (Mann-Whitney U test, p=0.08). MB post-dilatation improved malapposition in most scaffolds and there was a trend to further improvement with mini-KBPD.

Not surprisingly, SB ostial diameter **(Figure 4)** was closely related to SB balloon size across all SB angles (Kruskal-Wallis, p=0.007). In addition, the SB ostial diameter was maintained after MB post-dilatation and after mini-KBPD (Kruskal-Wallis, p=0.029 and p=0.032, respectively).

BALLOON DIAMETERS WITH MINI-KBPD AND KBPD

The proximal diameters (**Figure 1C**, **Figure 1D**) of balloons inflated with the mini-KBPD strategy (n=10) (2.91±0.08 mm) at 5 atm were less than with conventional KBPD (n=10) (4.21±0.10 mm, p=0.0001). The maximum diameters achieved with mini-KBPD and KBPD at 5 atm (5.09±0.08 and 5.07±0.08 mm, p=0.42) were similar.

In addition, elasticity of the phantom was confirmed because the proximal lumen which was 3.5 mm in diameter could be expanded to 4.21 mm with KBPD. It returned to its original diameter after balloon deflation.

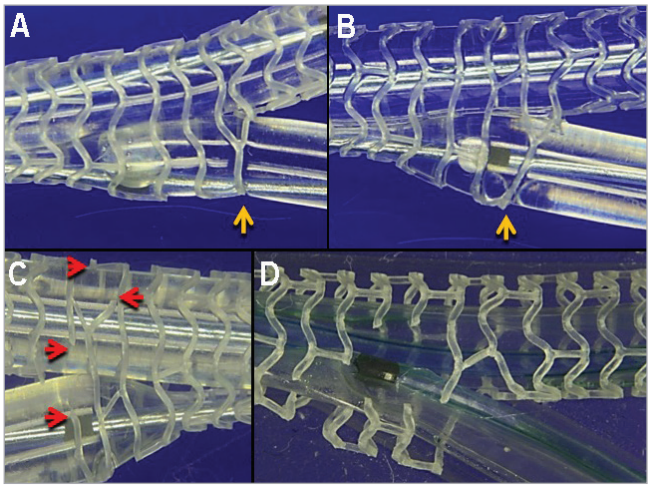

Figure 4. *Mini-KBPD at low (5 atm) and high (>15 atm) balloon pressures. Panel A is a photograph of mini-KBPD with 3.0 mm NC balloons inflated slowly to 5 atm in a 3.0 mm Absorb scaffold showing that there were no strut fractures. The yellow arrow indicates a strut that is restraining balloon expansion at this pressure. In panel B, the simultaneous balloon inflation pressure was increased to 15 atm in the same scaffold. The SB balloon had prolapsed forward ("melon seeding") and the scaffold strut no longer restrained balloon expansion because, as shown in panel C, struts had fractured (red arrows). The photograph D shows a scaffold severely damaged by high-pressure mini-KBPD with multiple fractures.*

Discussion

This study differs from other bench reports of Absorb scaffolds in bifurcations in that our study is quantitative as well as descriptive and we report more than 300 scaffold tests whereas others reported fewer than 10 tests[7,8]. The main findings were:

1. SB dilatation displaced struts from the SB ostium but distorted the MB scaffold **(Figure 1, Figure 5)**.
2. Either post-dilatation of the MB or post-dilatation of both branches with low pressure (5 atm) mini-KBPD largely resolved that distortion, without risk of strut fracture.
3. SB dilatation with a 3.0 mm non-compliant balloon in a 3.0 mm scaffold up to 10 atm pressure did not fracture struts. Above this threshold, with increasing pressure more strut fractures occurred. These fractures were usually single.
4. With low pressure (5 atm) mini-KBPD in a 3.0 mm scaffold with 3.0 mm NC balloons the scaffold constrained balloon expansion and fracture did not occur. Above 5 atm, the risk of fracture increased with increasing pressure.
5. With a single strut fracture there was no malapposition of this strut nor protrusion of the fractured strut into the phantom lumen.
6. Multiple strut fractures did occur at higher balloon pressures (>5 atm) with mini-KBPD. These were more likely to be malapposed and to project into the phantom lumen.

DISTORTION AND SCAFFOLD SB DILATATION

Scaffold SB dilatation aimed to displace struts from the SB ostium but caused distortion similar to that seen after metallic stent SB dilatation[6]. This distortion manifests as scaffold narrowing beyond the SB, scaffold malapposition opposite the SB and some protrusion of struts into the SB ostium **(Figure 1B)**.

The undesirable components of scaffold distortion can be largely corrected by MB post-dilatation or mini-KBPD. While on the bench we did not show a significant incremental benefit with mini-KBPD; in clinical practice, mini-KBPD has additional beneficial effects on carina shift and plaque distribution[11,13,14]. In patients, higher pressure sequential balloon inflation in the scaffold and in the branch may be needed to treat the underlying atheroma. The resulting distortion can be corrected safely by low-pressure mini-KBPD.

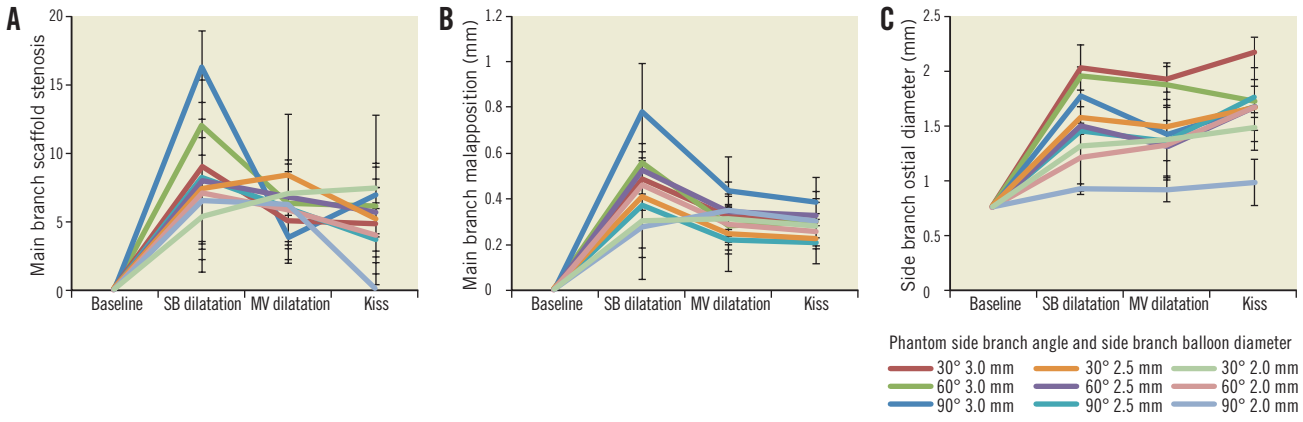

Figure 5. *Scaffold narrowing, main branch malapposition and side branch ostial scaffold diameter with side branch dilatation, main branch dilatation and mini-kissing balloon post-dilatation. Percentage scaffold narrowing (A), MB malapposition (B), and SB ostial diameter (C) at baseline, after SB dilatation of 3.0 mm scaffolds with 2.0, 2.5 or 3.0 mm balloons in phantoms with side branch angles of 30°, 60°, 90°. Findings after MB branch post-dilatation and after mini-KBPD are also shown. Three scaffolds were used for each series so that we assessed 27 scaffold dilatation sequences, hence 108 data points.*

SCAFFOLD INTEGRITY

The Absorb scaffold struts constructed from poly-L-lactic acid (PLLA)[15] compared with metallic struts have limited facility for post-dilatation without strut fracture[9]. Scaffold design influences the risk of strut fracture. The potential circular diameter of a cell in a 3.0 mm scaffold is 3.0 mm and that in a 3.5 mm scaffold is 3.6 mm, so that dilatation through the side of a 3.5 mm scaffold is less likely to cause damage than dilatation through the side of a 3.0 mm scaffold.

In the present study, SB dilatation of a 3.0 or 3.5 mm diameter Absorb at 14-16 atm with NC balloons caused strut fracture in 14% of 145 SB dilatations. The 2.0 mm balloon did not cause strut fracture **(Table 1)** and there was a trend for a 3.0 mm balloon to cause more strut fracture (19%) than a 2.5 mm balloon (13%, p=0.3713). The incidence of connector fracture (8% of dilatations) was similar to the incidence of hoop fracture (6%, p=0.643) despite connectors being narrower in a circumferential direction than hoops **(Figure 1)** so that they might be expected to fracture more readily than hoops.

The current study draws attention for the first time to the relationship between inflation pressure and strut fracture. Mini-KBPD with two 3.0 mm NC balloons inflated simultaneously in a 3.0 mm scaffold at low pressure (<5 atm) did not cause fracture. The balloons showed "waisting" as the scaffold constrained their expansion at low pressure **(Figure 4)**. Above a 5 atm threshold the likelihood of strut fracture increased with increasing inflation pressures **(Figure 3)**. Similarly, SB dilatation with a single 3.0 mm balloon in a 3.0 mm scaffold was associated with an increase in the likelihood of strut fracture beyond a threshold of 10 atm **(Figure 3)**. With single fractures, there was generally no strut protrusion into the lumen. At high pressures the fractures could be multiple, with the ends of fractured struts malapposed, overlapping and projecting into the lumen, creating a likely substrate for adverse clinical events **(Figure 4)**.

Other factors which may influence the potential for fracture include the age of the scaffold and the rapidity of balloon expansion.

CLINICAL DEPLOYMENT AND POST-DILATATION STRATEGY WITH ABSORB SCAFFOLDS

Trials evaluating metal stents in bifurcation disease have shown that, for most lesions, one stent is better than two[11,16], and it is likely that a single scaffold strategy would also be better than a more complex approach. When deploying a scaffold across an SB, we follow the EBC recommendations for metallic stents[11], except that we size the scaffold to the proximal rather than distal vessel diameter to reduce the chance of proximal scaffold overdilation and strut damage **(Figure 2)**. After optimal MB stent expansion, the decision needs to be made whether or not to carry out KBPD. With metal stents and normal SB flow, the Nordic-Baltic III study found no difference in major clinical events between those who did and those who did not have routine KBPD[17]. KBPD was, however, associated with reduced SB angiographic restenosis at the expense of a longer procedure and greater contrast use.

In addition, KBPD or mini-KBPD may be beneficial because they open struts, potentially facilitating subsequent SB access.

While we aim for a single scaffold strategy, sometimes KBPD fails to provide a satisfactory outcome. Then the cardiologist may decide to treat the SB with a stent (or scaffold). We are currently studying provisional SB strategies, and the best strategy is likely to be T-stenting with a metallic drug-eluting stent in the SB.

SCAFFOLD LATE OUTCOMES

The Absorb scaffold behaves in unique ways that will probably impact on late outcomes after implantation in bifurcations. While full absorption takes three to four years[18], by one year there is sufficient programmed loss of scaffold integrity that the vessel is no longer splinted, allowing vessel and scaffold positive remodelling[19]. How this enlargement may influence bifurcation scaffolding is unknown. Those patients from Cohort B of the ABSORB study with a scaffold deployed across an SB were followed by serial 3D optical coherence tomography. The scaffold divided the SB ostium into compartments. The number of compartments and average ostial area free from struts did not change from baseline to six months, but then significantly reduced from six months to two years due to tissue growing between the struts. However, the ostial area free of struts increased between 12 months and three years without change in compartment number, possibly due to regression of intimal hyperplasia. It is interesting to speculate that beyond three years the ostium may become unobstructed because the scaffold has resorbed, intimal hyperplasia has regressed and positive remodelling has occurred.

Study limitations

Although bench testing provides valuable insights that may improve clinical practice, it uses models that simplify the *in vivo* situation and may not accurately predict scaffold behaviour in human subjects. The silicone models do have elasticity, but how closely this corresponds to human conditions is unknown. While in the phantom, single fractures did not prolapse into the lumen; this may not be true *in vivo*. Our phantom design did not correspond to fractal geometry. The study findings need to be confirmed *in vivo*.

Summary

Dilatation through the side of an Absorb scaffold causes distortion similar to that seen after dilatation through the side of a metallic stent. The undesirable aspects of SB dilatation (MB scaffold narrowing and scaffold malapposition) can be corrected by mini-KBPD without loss of desirable aspects (clearance of struts from the SB). Inflation of a 3.0 mm balloon to a threshold of 10 atm through the side of a 3.0 mm scaffold is safe, without causing strut fracture. At higher pressures, there is an increased chance of strut fracture. With mini-KBPD with 3 mm balloons in a 3.0 mm scaffold, the safe inflation pressure threshold without strut fracture is 5 atm, which is sufficient to correct MB distortion. At higher pressure mini-KBPD, there is an increasing risk of strut fracture. These benchtop insights may help guide the clinical deployment of Absorb scaffolds in bifurcations and might enhance clinical outcomes.

The best strategy for deployment of an Absorb scaffold in most bifurcation lesions is likely to be a provisional approach. The scaffold proximal to the SB can be optimally expanded by post-dilatation with a balloon sized to the proximal vessel. If there is impaired flow or a severe stenosis in the SB, SB dilatation followed by mini-KBPD may be considered. Optimal techniques for use of Absorb in bifurcations need to be determined by clinical trials.

Impact on daily practice

This paper studies dilatation through the side of Absorb scaffolds and how best to postdilate scaffolds. Side branch dilatation causes distortion similar to that in a metallic stent. Daily practice is impacted because this distortion is best corrected by mini-kissing balloon post-dilatation (small overlap of simultaneously inflated balloons). Dilatation can cause scaffold strut fractures and our bench tests may predict safe clinical practice. Side branch dilatation of a 3.0 mm scaffold with a 2.0 mm balloon did not cause strut fractures. Side dilatation with a 3.0 mm balloon at 10 atm or less did not cause strut fractures. Mini-kissing balloon dilatation of a 3.0 mm scaffold with two 3.0 mm balloons at 5 atm or less did not damage scaffolds. At higher pressures, multiple fractures could occur.

Funding

Testing was funded by the Auckland Heart Group Charitable Trust. Some scaffolds were supplied by the manufacturer.

Conflict of interest statement

J. Ormiston is an advisory board member for Abbott Vascular and Boston Scientific and has received minor honoraria from them. The other authors have no conflicts of interest to declare.

References

1. Ormiston J, Serruys PW, Regar E, Dudek D, Thuesen L, Webster M, Onuma Y, Garcia-Garcia H, McGreevy R, Veldhof S. A bioabsorbable everolimus-eluting coronary stent system for patients with single de-novo coronary artery lesions (ABSORB): a prospective open-label trial. *Lancet.* 2008;371:899-907.

2. Serruys PW, Ormiston J, Onuma Y, Regar E, Gonzalo N, Garcia-Garcia H, Nieman K, Bruining N, Dorange C, Miquel-Hebert K, Veldhof S, Webster M, Thuesen L, Dudek D. A bioabsorbable everolimus-eluting coronary stent system (ABSORB): 2-year outcomes and results from multiple imaging methods. *Lancet.* 2009;373:897-910.

3. Okamura T, Onuma Y, Garcia-Garcia H, Regar E, Wykrzykowska J, Koolen J, Thuesen L, Windecker S, Whitbourn R, McClean D, Ormiston J, Serruys PW; ABSORB Cohort B Investigators. 3-Dimensional optical coherence tomographic assessment of jailed side-branches by bioresorbable scaffolds: a proposal for classification. *JACC Cardiovasc Interv.* 2010;3:836-44.

4. Gogas B, van Geuns R, Farooq V, Regar E, Heo J, Ligthart J, Serruys P. Three-dimensional reconstruction of the post-dilated ABSORB everolimus-eluting bioresorbable vascular scaffold in a true bifurcation lesion for flow restoration. *JACC Cardiovasc Interv.* 2011;4:1149-50.

5. Ormiston J, Webster M, Ruygrok P, Stewart J, White H, Scott D. Stent deformation following simulated side-branch dilatation: a comparison of five stent designs. *Catheter Cardiovasc Interv.* 1999;47:258-64.

6. Grundeken M, Kraak R, de Bruin D, Wykrzykowska J. Three-dimensional optical coherence tomography evaluation of a left main bifurcation lesion treated with an ABSORB® bioresorbable vascular scaffold including fenestration and dilatation of the side branch. *Int J Cardiol.* 2013;168:e107-8.

7. Dzavik V, Colombo A. The absorb resorbable scaffold in coronary bifurcations: insights from bench testing. *JACC Cardiovasc Interv.* 2014;7:81-8.

8. Sguelia G, D'Errico F, De Santis A, Gaspardone A. First ad hoc bioresorbable vascular scaffold bench test: a glimpse into percutaneous bifurcation interventions. *Int J Cardiol.* 2014;172:604-6.

9. Ormiston J, De Vroey F, Serruys PW, Webster M. Bioresorbable polymeric vascular scaffolds: a cautionary tale. *Circ Cardiovasc Interv.* 2011;4:535-8.

10. Louvard Y, Dzavik V, Hildick-Smith D, Galassi A, Pan M, Burzotta F, Zelizko M, Dudek D, Ludman P, Sheiban I, Lassen J, Darremont O, Kastrati A, Ludwig J, Iakovou I, Brunel P, Lansky A, Meerkin D, Legrand V, Medina A, Lefevre T. Classification of coronary artery bifurcation lesions and treatments: time for a consensus! *Catheter Cardiovasc Interv.* 2008;71:175-83.

11. Hildick-Smith D, Lassen J, Albiero R, Lefevre T, Darremont O, Pan M, Ferenc M, Stankovic G, Louvard Y; European Bifurcation Club. Consensus from the 5th European Bifurcation Club meeting. *EuroIntervention.* 2010;6:34-8.

12. Ormiston J, Webster M, Webber B. Percutaneous intervention for coronary lesions: Bench testing in the real world, in Waksman R, Ormiston J, eds. Bifurcation Stenting. West Sussex, UK: Wiley-Blackwell; 2012. p.83-88.

13. Rahman S, Leesar T, Cilingiroglu M, Effat M, Arif I, Helmy T, Leesar M. Impact of kissing balloon inflation on the main vessel stent volume, area, and symmetry after side-branch dilation in patients with coronary bifurcation lesions: a serial volumetric intravascular ultrasound study. *JACC Cardiovasc Interv.* 2013;6:923-31.

14. Louvard Y, Lefèvre T, Morice MC. Percutaneous coronary intervention for bifurcation coronary disease. *Heart.* 2004;90:713-22.

15. Ormiston J, Webster M, Armstrong G. First-in-human implantation of a fully bioabsorbable drug-eluting stent: the BVS poly-L-lactic acid everolimus-eluting coronary stent. *Catheter Cardiovasc Interv.* 2007;69:128-31.

16. Steigen T, Maeng M, Wiseth R, Erglis A, Kumsars I, Narbute I, Gunnes P, Mannesverk J, Meyerdierks O, Roevatn S, Niemela M, Kervinen K, Jensen J, Galloe A, Nikus K, Vikman S, Ravkilde J, James S, Aoroe J, Ylitalo A, Helqvist S, Sjogren I,

Thayssen P, Virtanen K, Puhakka M, Airaksinen J, Lassen J, Thuesen L; Nordic PCI Study Group. Randomized study on simple versus complex stenting of coronary bifurcation lesions: the Nordic bifurcation study. *Circulation*. 2006;114:1955-61.

17. Niemela M, Kervinen K, Erglis A, Holm N, Maeng M, Christiansen E, Kumsars I, Jegere S, Dombrovskis A, Gunnes P, Stavenes N, Steigen T, Trovic T, Eskola M, Vikman S, Pomppanen H, Makikallio T, Hansen K, Thayssen P, Aberge L, Jensen L, Hervold A, Airaksinen J, Pietila M, Frobert O, Kellerth T, Ravkilde J, Aaroe J, Jensen J, Helqvist S, Sjogren I, James S, Miettinen H, Lassen J, Thuesen L; Nordic-Baltic PCI Study Group. Randomized comparison of final kissing balloon dilatation versus no final kissing balloon dilatation in patients with coronary bifurcation lesions treated with main vessel stenting: the Nordic-Baltic Bifurcation Study III. *Circulation*. 2011;123:79-86.

18. Onuma Y, Serruys PW, Perkins L, Okamura T, Gonzalo N, Garcia-Garcia H, Regar E, Kamberi M, Powers J, Rapoza R, van Beusekom H, Van der Giessen W, Virmani R. Intracoronary optical coherence tomography and histology at 1 month and 2, 3, and 4 years after implantation of everolimus-eluting bioresorabable scaffolds in a porcine coronary artery model: an attempt to decipher the human optical coherence tomography images in the ABSORB trial. *Circulation*. 2010;122:2288-300.

19. Ormiston J, Serruys PW, Onuma Y, van Geuns R, de Bruyne B, Dudek D, Thuesen L, Smits P, Chevalier B, McClean D, Koolen J, Windecker S, Whitbourn R, Meredith I, Dorange C, Veldhof S, Hebert KM, Rapoza R, Garcia-Garcia H. First serial assessment at 6 months and 2 years of the second generation of absorb everolimus-eluting bioresorbable vascular scaffold: a multi-imaging modality study. *Circ Cardiovasc Interv.* 2012;5:620-32.